Selective extraction of lithium from seawater desalination concentrates: Study of thermodynamic and equilibrium properties using Density Functional Theory (DFT)

R. Coterillo [a], L.-E. Gallart [b], E. Fernández-Escalante [b], J. Junquera [a], P. García-Fernández [a], I. Ortiz [b], R. Ibañez [b], M.-F. San-Román [b,*]

[a] Dpto. de Ciencias de la Tierra y Física de la Materia Condensada, Facultad de Ciencias, Universidad de Cantabria, Avda. de los Castros, 48, Santander 39005, Cantabria, Spain
[b] Dpto. de Ingenierías Química y Biomolecular, ETSIIyT, Universidad de Cantabria, Avda. de los Castros, 46, Santander 39005, Cantabria, Spain

HIGHLIGHTS

- Selective extraction of lithium from seawater desalination concentrates
- The most promising of extractants, β-diketones and organophosphates were selected.
- Electrostatic interaction confirmed using square of electronic wave function
- Thermodynamic and equilibrium parameters gotten by Density Functional Theory (DFT)
- Best selectivity of Li$^+$ obtained using DBM•TOPO and LIX54•TOPO systems

GRAPHICAL ABSTRACT
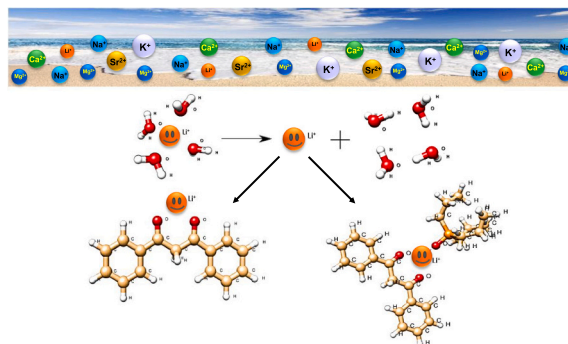
ARTICLE INFO

ABSTRACT

Lithium, declared critical raw material by the European Union in 2020, is a competitor to hydrogen as alternative to petroleum. Its use is increasing while reserves are declining, boosting new sources, as seawater desalination concentrates. In this work, a computational study of the most promising extractants, β-diketones and organophosphates and combinations thereof, towards lithium in presence of metal ions found in the concentrates, Na$^+$, K$^+$, Mg^{2+}, Ca^{2+} and Sr^{2+} was carried out, via molecular simulation using ab initio Density Functional Theory (DFT). The geometries, reaction energies, and thermodynamic parameters have been evaluated. Using the square of the electronic wave function an electrostatic interaction was confirmed as cation-extractant/s bonding. The complexation reaction energies of the systems formed by a cation and a single extractant display negative ΔE and ΔG values, pointing towards stable complexes and spontaneous reactions. The synergic effect of extractants was studied by combining the β-diketones with TOPO (1:1) leading to an increase of ΔE and ΔG (absolute value). The extraction coefficient, K, follows the order $K(K^+) > K(Na^+) > K(Li^+) > K(Sr^{2+}) > K(Ca^{2+}) > K(Mg^{2+})$. In consequence, selectivity Li$^+$ towards cations of the group II was higher, $S(Li^+/Mg^{2+}) > S(Li^+/Ca^{2+}) > S(Li^+/Sr^{2+})$ for the combined mixtures BTA•TOPO and FDOD•TOPO and lower towards group I cations, $S(Li^+/Na^+) >$

* Corresponding author.
E-mail address: sanromm@unican.es (M.-F. San-Román).

S(Li$^+$/K$^+$) for DBM•TOPO and LIX54•TOPO. The selectivity of Li$^+$ regarding the rest of the cations and the 16 extractants and mixtures of extractants was lower than the selectivity of Li$^+$ with respect to each cation, being the best value for the DBM•TOPO and LIX54•TOPO systems. The results obtained are expected to provide a tool on the behaviour of the most promising of extractants towards Li$^+$ in seawater desalination concentrates.

1. Introduction

Lithium, the lightest metallic element, is the 25th most abundant element on Earth. Due to its excellent properties, such as a low thermal expansion coefficient and the highest redox potential and specific heat capacity of any solid element [1], it has become a very coveted material in the worldwide industrial scenery, mainly in lithium-ion battery manufacture (71%), but also in ceramics and glass (14%), lubricating greases (4%), polymer production (2%), continuous casting mold flux powders (2%), air treatment (1%) and other uses (6%) [2]. The rapid development of electric vehicles and the increasing use of portable electronic devices has greatly increased Li consumption worldwide, achieving 57,700 tons in 2019, 18% higher than in 2018 [3].

Lithium sources can be classified into mineral sources and aqueous sources, as salt lake brines and seawater. Lithium extraction from minerals is costly and environmentally damaging due to its complex production process and high energy and acid consumption [4]. Lithium produced worldwide is obtained mainly from salt lake brines [1], with the cost of production from this source being 30%–50% lower than from ores [5]. The current process to recover lithium from salt lake brines, known as evaporitic technology, has certain disadvantages such as long water evaporation times through solar and wind evaporation (over a year), consumption of large amounts of water due to the evaporation process, which affects the hydrological water cycle and is strongly dependent on weather conditions. Li recovery with this process is approximately 70%, being in some brines 50% or even lower values [6]. On the other hand, although the ocean contains large amounts of lithium, it is found in very low concentrations (average 0.17 mg/L) to be exploited in the short term [6].

The increasing industrial demand for lithium has fueled the quest to find new viable sources, such as brines obtained from seawater desalination plants [7–9]. The growing interest in the sustainability of desalination processes, to reduce the impact generated by the discharge of brine, and the revaluation of this saline waste as raw material, has led to the development of processes aimed at the material valorization of SWRO desalination brines by means of the recovery of different materials. Although Lithium concentration in SWRO desalination brines is lower than in other conventional sources, the high volume of brine generated in the world and the growing trend forecasted for the coming years, and the increasing need to find new supply sources of this critical material, foster the research and development of strategies for the recovery of lithium from this unconventional source. Their increased Li$^+$ concentration over seawater, as well as its contribution to the transition towards a circular economy, makes it an attractive alternative for Li$^+$ recovery. Current global brine production in desalination plants worldwide stands at 141.5 million m^3/day, totaling 51.7 billion m^3/year [10]. Even so, it is a challenge to incorporate technologies capable of extracting Li$^+$ due to its still low concentration and the competence of other ions. The most studied ones to date are precipitation [11,12], ion exchange adsorption [7,13,14], membrane separation (nanofiltration) [15–17], electrochemical methods [18,19] and liquid-liquid extraction [20–23]. The precipitation method is just suitable for brine with high lithium ion concentrations (like lake brines with concentration Li$^+$ around 6.000 mg/L). On the other hand, the stability and selectivity of the adsorption method are still low, not enough to achieve industrial production. With regard to membrane separation, it is suitable for solutions with very low ion concentration, such as extraction of lithium ions from seawater, while electromembrane processes are still intensive from an energy point of view. Liquid-liquid extraction, our leading

focus, has certain advantages such as low cost, high efficiency, easy scalability, simple equipment requirements and recyclable extractants [1,24,25].

The most common compounds for lithium extraction may be classified into acidic extractants (organophosphates and carboxylics), ionic liquids, chelating agents (crown-ethers and β-diketones) and solvating extractants (organophosphates and β-diketones) [1,26]. Acidic extractants (di-(2-ethylhexyl)phosphoric acid (D2EHPA), Versatic Acid 10, etc.) present a problem in that they are more selective to divalent ions than monovalent ones, since their extraction mechanism relies on ionic exchange [22,27,28]. Extraction with ionic liquids (ILs) also exhibits similar issues, as in this case the reaction takes place by exchange of Li$^+$ with the cationic counterpart of the ionic liquid, involving extractant losses along the way [26,29]. In addition, they are expensive and highly viscous compared to organic solvents. On the other hand, corona ethers (CEs) (14-crown-ether derivatives and 12-crown-4 [23,30]) are polyethers with a ring structure, whose bonding mechanism is dominated by electrostatic interactions [26]. These compounds present a cavity at the nanometer scale, which allows the formation of a compound with optimal stability when its size and that of the cation are similar [1], rendering them unable to differentiate between Li$^+$ and Mg^{2+} due to their similar ionic radius [26]. The most common organophosphates solvating extractants (SEs) are trioctylphosphine oxide (TOPO) and tributyl phosphate (TBP) [20,31,32] but it has been shown that this type of extractant alone has a negligible extraction efficiency [31]. Therefore, a co-extractant is usually added to these extractants to improve extraction efficiency and Li$^+$ selectivity. TBP-FeCl$_3$, the most studied of such systems, has several disadvantages such as the addition of iron, and a poor stability of the organic phase that leads to extractant loss in the aqueous phase [33]. Similarly, other co-extractants such as sodium tetraphenylborate (NaBPh$_4$), potassium hexafluorophosphate (KPF$_6$) and sodium phosphomolybdate (Na$_3$PMo$_{12}$O$_{40}$) all have in common that they add one of the other metal ions present in seawater, and hence work against a selective extraction [20,34,35]. Cyanex 923, a mixture of trialkyl-phosphine oxides, has been successfully used to selectively extract Li$^+$ with respect to Na$^+$ in combination with some β-diketones (1-heptyl-3-phenyl-1,3-propanedione (LIX54) [36,37]. However, when used in combination with other β-diketones (4-benzoyl-3methyl-1-phenyl-2-pyrazolin-5-one (PMBP), Mextral EOL (basically LIX54)), it has been found to selectively extract Mg^{2+} over Li$^+$ [21,38]. Another family of solvent extractants have been studied for Li$^+$ extraction, such as the new deep eutectic solvents (DESs) (tetrabutylammonium chloride (TBAC) + oleic acid (OA) [31,36]). However, their application in liquid-liquid extraction processes has been difficult due to their hydrophilicity [31]. Kurniawan et al. [39] used a calix[4]arene derivative which, in addition to its high price, presented slow kinetics that made it inefficient in a liquid-liquid extraction setup. Katsuta et al. [40] employed a synthetic compound [Ru(3,5-dimethylanisole)(pyO$_2$)$_3$], where it was found that even in the presence of Ca^{2+} and Mg^{2+} the Li$^+$ extraction was 99%, but 4% of it was lost in the scrubbing process. Finally, the already mentioned β-diketones, characterized by the presence of two ketone groups, are able to extract Li$^+$ by means of Pearson's principle [26,41]. Some examples among the bibliography are 2-thenoyltrifluoroacetone (TTA), benzoyltrifluoroacetone (BTA), heptafluoro-dimethyloctanedione (FDOD), 4,4,4-trifluoro-1-(2-furyl)-1,3-butanedione (FTA), dibenzoylmethane (DBM), 2-naphthoyltrifluoroacetone (NTA), 2,9-dimethyl-1,10-phenanthroline (DMP) and 1,10-phenanthroline (PHEN). It should be noted that the state of the art shows that β-diketones and organophosphate extractants have a feasible Li$^+$ re-

extraction stage using HCl [31,37,41].

Most of the experimental data in open literature have been carried out in synthetic solutions or brines in which Sr^{2+} is not found. Moreover, most only include the alkali metal ions found in the brines, and at the time of this writing, there are no experimental results where all six metal ions are present at the same time, particularly it is necessary to find lithium-selective extractants in such complex mixtures, especially with respect to Mg^{2+}, since their similar ionic radius makes their separation more difficult [42].

The main objective of this work is to carry out a computational study of the most promising of those extractants towards lithium in presence of the metal ions found in higher concentrations in the brines such as Na^+, K^+, Mg^{2+}, Ca^{2+} and Sr^{2+} was carried out. For this, their equilibrium and thermodynamic properties have been obtained via molecular simulation using ab initio Density Functional Theory (DFT) simulations. The results obtained from these simulations will hopefully yield some predictive power on the behaviour of these extractants when it comes to practical Li^+ extraction and thus reducing the experimental work required in these studies.

2. Computational model

2.1. Conceptual development

In a general chemical reaction the reaction energy ΔE is defined as the difference between the sum of energies of the reagents and that of the products:

$$\Delta E = \sum E_{products} - \sum E_{reagents} \qquad (1)$$

each of them being in its optimized geometry. Negative values of the reaction energy indicate stable reaction products. In general, the larger the value (absolute) the higher the stability. This value, however, only yields information about the molecule at a temperature of $T = 0$ K, i.e. frozen. In order to introduce thermal effects one may use the vibrational frequencies ω_i of the system, typically in conjunction with an ideal molecular gas model [43], to infer the activation of the molecular vibrational modes and hence obtain the zero-point energy E_{ZPE} and the entropy S of the system at a given temperature T. A self-consistency cycle -or single point calculation- of density functional theory (DFT) provides the internal energy E of a given system, with an accuracy dictated by choice of functional and the characteristics of the molecule at hand [44]. One may use several of these energy calculations to perform a geometry optimization of the molecule, a procedure whereby its energy is minimized in terms of its atomic coordinates through various numerical methods, such as conjugated gradient descent (CGD). Additionally, in order to ensure the stability of the optimized geometry -i.e. to confirm whether it is indeed a local energy minimum or just a saddle point the potential energy surface (PES) of the molecule, and hence subject to deformations- one may obtain the Hessian or dynamical matrix of the system through a finite-difference approach. The diagonalization of the matrix yields the vibrational modes of the molecule as eigenvectors, and the corresponding frequencies ω_i as the associated eigenvalues. If all frequencies turn out positive, then the structure is stable. Otherwise, a lower energy structure may be obtained by deforming the molecule in the 'direction' of the vibrational mode with the highest negative frequency and repeating the optimization process until all frequencies are positive [45]. With said thermodynamic values one may obtain the free energy, G, of the system in the gas phase:

$$G_{gas} = (E + E_{ZPE}) - TS = E_0 - TS \qquad (2)$$

However, to accurately represent the proposed computational study, the effects of the liquid phase on the reagent to be extracted must be accounted. In classical molecular dynamics simulations, this is usually done by submerging the molecule in a box full of solvent molecules and performing some sort of statistical average. Alas, the computational cost

of fully-fledged quantum mechanical calculations renders this approach unfeasible. Hence, in this work, it was introduced an implicit solvation. These kinds of models generate a charged surface around the molecule based on its electronic density, and emulates its interaction with a continuum-like solvent. The model provides a correction to the free energy of solvent, G_{sol}, which may be combined with the gas phase result to obtain the free energy in the liquid phase.

$$G = G_{gas} + G_{sol} \qquad (3)$$

Similarly, to the aforementioned reaction energy, one may define a general reaction free energy as:

$$\Delta G = \sum G_{products} - \sum G_{reagents} \qquad (4)$$

A negative value of ΔG would imply the reaction occurs spontaneously at the considered temperature. Finally, the reaction free energy may also be used to calculate the equilibrium constant k_e of the reaction as follows:

$$k_e = exp\left(-\frac{\Delta G}{RT}\right) \qquad (5)$$

2.2. Extraction model

The extraction power of an extractant for metal ions was investigated based on the previously described reaction energies (Eq. (1)) as a measure of the stability of the cation-extractant system, that is to say as a measure of the stability of the final complex according to complexation reaction of the form:

$$A^{m+} + L \leftarrow - \rightarrow [A^{m+} \bullet L] \qquad (6)$$

where A^{m+} is the cation and L denotes the chosen extractant. In this sense, the reaction energy may also be understood as the bonding energy between the cation and the extractant. On the other hand, it was also looked at the hydration process of the cations, as they are the competing reactions in the extraction processes [30]. The hydration reaction between a cation and the n water molecules within its coordination shell may be written as:

$$A^{m+} + nH_2O \leftarrow - \rightarrow \left[A(H_2O)_n\right]^{m+} \qquad (7)$$

Finally, the extraction model was characterized by defining a coefficient of extraction K as the ratio between the equilibrium constants of the complexation (k_{ec}) and hydration (k_{eh}) reactions.

$$K = \frac{k_{ec}}{k_{eh}} \quad ln(K) = \ln(k_{ec}) - \ln(k_{eh}) \qquad (8)$$

The fact that there is not a general agreement in the number of water molecules in the coordination shell of the cations [46] involves one of the major approximations in this model, that undoubtedly affects the results of the calculations [47]. In this work, a value of $n = 4$ was selected arbitrarily for all cations, as it is the most accepted coordination number for the Li^+ cation [46]. However, it is a worst-case scenario for lithium extraction, as the hydration enthalpy of the larger cations, that would otherwise bond more strongly, is underestimated. Additional water molecules around Na^+, K^+, Mg^{2+}, Ca^{2+} and Sr^{2+} would give rise to a greater k_{eh} and according to Eq. (8), a lower equilibrium constant of the complexation, K. Using higher coordination numbers supposes complex computational calculations that entail a high cost of computation, that is why $n = 4$ was considered a valid choice for comparison purposes.

Additionally, in order to assess how a given extractant preferentially extracts a cation over the others, the selectivity of an extractant towards a given cation S was defined:

$$S_{A_i^{m+}} / \sum_{A_j^{m+}} = \frac{\left(K_{A_i^{m+}}\right)}{\sum \left(K_{A_j^{m+}}\right)} \tag{9}$$

where A_i^{m+} is a metal ion of interest and A_j^{m+} is the rest of the metal ions present in the aqueous solution.

2.3. Computational details

The starting structures of the extractant and cation-extractant complexes were hand-crafted with the Avogadro chemical editor and they were built-in UFF force field potential [48,49]. Structural optimizations were carried out using the ORCA 4.2.1 quantum chemistry package [50] at the B3LYP/def2-SVP level of theory [51,52]. This includes both the optimization process and the later frequency calculation. Furthermore, an additional single-point calculation at the B3LYP/def2-QZVP level was performed on the optimized structures so as to ensure accurate energy values. This same functional had been previously applied to the binding of cations to crown ethers [30,53], and it was further validated through comparison with separate second-order Møller–Plesset theory calculations (MP2) in one of the systems [54].

The effects of the solvation media—i.e. the kerosene-based organic phase on the bonding process were considered through the inclusion of the Solvation Model based on Density (SMD), developed by Marenich et al. [55], in the final energy calculations of the cation-extractant reactions. Geometry optimizations and frequency calculations, however, were performed without the implicit solvent model, as tests indicated that the final geometries remained largely unaffected and the numerical noise introduced by this approach would render the molecular PES too unstable to find reliable minima, partly due to the large size of the systems. It was also omitted in the case of the hydration reactions, as the solvent is already considered explicitly in the reaction itself.

Grimme's D3 dispersion correction [56] for non-covalent interactions, usually overlooked by DFT functionals, and the RIJCOSX integral approximation [57,58] using the highest integration grid setting available, were included in all calculations so as to optimize the accessible computational resources. The Multiwfn software [59] was used to perform an electronic density-based topological analysis of the atomic charges (also known as Atoms in Molecules (AIM) or Bader charge analysis [60]), as well as to generate the electronic density diagrams of the following sections. Finally, when the extractants studied in this work present long carbon chains, it is expected to have little to no effect in the bonding process, and hence were cut at a length of three carbon atoms in order to reduce computational costs. This approximation was tested by looking at the reaction free energy and the $A^{m+} \bullet O$ distance in the complexation of the $A^{m+} \bullet L$ system while varying the length of the carbon's chain. It was obtained discrepancies of less than 1.0 kcal/mol with respect to the full chain, introducing an error far inferior to that introduced by other assumptions. As an example, Fig. 1 shows the ΔG for the complex $Li^+ \bullet TOPO$ and the $Li^+ \bullet O$ distance (oxygen from the phosphate group of the extractant). As can be seen, from 3 carbons in the linear chain of the extractant, the variation of ΔG and the $Li^+ \bullet O$ distance is negligible.

The detailed computational procedure was applied to a target of extractant candidates selected as a result of a deep revision of the available literature focused on lithium extraction from ideal and real seawater desalination concentrates.

3. Results and discussion

It is known that the combination of solvating extractants such as TBP or TOPO with β-diketones (TTA or BTA) presents a synergistic effect on Li^+ extraction [31,41,61,62]. In these cases, it is thought that the β-diketone forms a chelating complex with the metal ion and the neutral extractant displaces the remaining water molecules to improve the
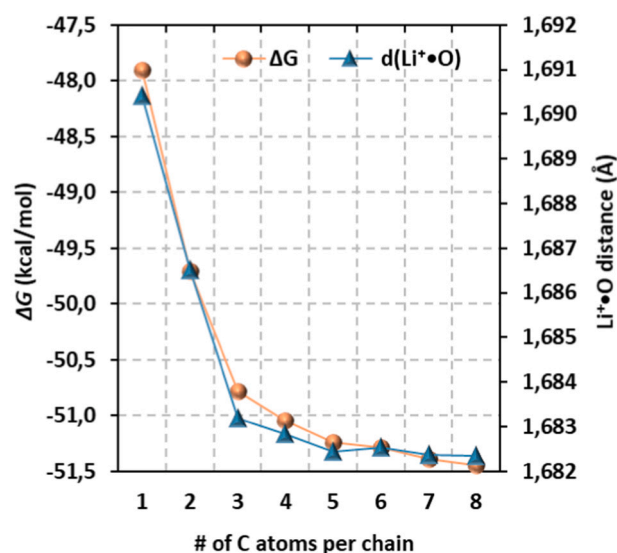
Fig. 1. Reaction free energy, ΔG, and $Li^+ \bullet O$ distance in the complexation of the $Li^+ \bullet TOPO$ system complexation versus the length of the carbon chains in the TOPO extractant.

solubility of the complex in the organic phase [63]. These studies have been performed mostly in the presence of other alkali metal ions (Na^+, K^+) only, and when Ca^{2+} and Mg^{2+} have been found the concentrations were very small. In the presence of alkali metal ions it is seen that this mixture of extractant types is selective to Li^+ and reaches high extraction values (mostly 96%–99%). In these cases, the most employed β-diketone has been TTA and the most employed neutral extractants TBP and TOPO, but the combination of β-diketone with the latter presents higher extraction efficiency [41,62,64]. Harvianto et al. [62] took alkaline earth metal ions into account in a pairwise extraction study, where it is observed that even at high concentrations of K^+, Na^+ and Ca^{2+} more than 70% Li^+ extraction is obtained, but at high concentrations of Mg^{2+} it decreases drastically to 10%. Most of the references found in our study of the state of the art only include monovalent cations. Nevertheless, divalent cations are the main competitors in lithium extraction; this study has considered not only monovalent cations (Li^+, Na^+, K), but also divalent cations Ca^{2+}, Mg^{2+} and even Sr^{2+}, which are not usually included in this type of mixture. Besides the additional complexity added, this study aims at obtaining results that are closer to the reality when working with saline brines.

As described in the literature, in view of their higher selectivity and their extraction mechanism towards Li^+, in this study both solvating extractants and β-diketones -as well as mixtures thereof-, have been selected as targets for computational study. In particular, the β-diketones DBM, TTA, FTA, BTA, FDOD and LIX54 as well as the organophosphates TOPO, TBP, TRIS and BIS were chosen as candidate extractants. Combinations of β-diketones with TOPO were also considered so as to assess their synergistic behaviour, as well as the different combinations of β-diketones with TOPO and an $n = 4$ tetrahedral hydration shell. Each of these systems was combined with the group I (Li^+, Na^+, K^+) and group II (Mg^{2+}, Ca^{2+}, Sr^{2+}) cations in order to assess their binding energies, making for a total of 96 complexations and 6 hydration reactions. Most bibliographic sources usually work with very aggressive pH values in order to protonate the system and force a proton-cation exchange with the extractants. This study took into account a working pH value below the pKa of each extractant in order to consider a neutral and non-protonated system. In this configuration, the cations are located next to the corresponding oxygen atom(s) while that if the system is protonated, it non-selectively extracts to all cations, Li^+, Na^+, K^+, Mg^{2+}, Ca^{2+}, Sr^{2+}.

A summary of the available literature on the experimental

Table 1
Summary of the available literature for the selected extractant candidates.

Source	Extractants	Metal ion concentration (g/L)	Results (% extraction, etc.)	Ref.
Synthetic solution	TBP, TRIS, BIS	a) Li^+ 0.026, Mg^{2+} 0.091 b) Li^+ 0.416, Na^+ 1.38, K^+ 2.35	• Best results: TBP a) Li^+ 100%, Mg^{2+} 0% b) Li^+ 42.6%, Na^+ 26.2%, K^+ 38.7%	[32]
Synthetic salt lake brine	TTA•TOPO	Li^+ 1.17, Na^+ 129.6, K^+ 40.9	• Li^+ 95.7%, Na^+ 1.1%, K^+ < 0.01%	[31]
Synthetic solution	FDOD•TOPO	Li^+ 0.000694	• Supported liquid membrane studies Li^+ > 99%	[65]
Synthetic solution	FTA•TOPO	Li^+ 1.0	• Analyses kinetics and mechanisms of extraction. Process controlled by the chemical reaction at the interface	[66]
Synthetic ammoniacal solution	TTA•TOPO	Li^+ 0.16	• Li^+ 97.13%	[64]
Alkaline brines from lithium carbonate precipitation process	BTA•TOPO	Li^+ 2, Na^+ 49.9, K^+ 1.02, Mg^{2+} 0.005, Ca^{2+} $5 \cdot 10^{-4}$	• Li^+ 96%, 7 stage mixer-settler, Na^+/Li^+ molar ratio reduced from 7.98 to 0.008, impurities of K^+, Ca^{2+}, Mg^{2+} < 0.1 g/L	[41]
Concentrated seawater from the desalination process and seawater	TTA•TOPO	n.d.	• Seawater: Li^+ 65% Concentrated seawater: Li^+ ~ 58%	[67]
Synthetic solution	TTA, DBM, TBP, TOPO	Li^+ 0.001, Na^+ 10, K^+ 0.4, Mg^{2+} 1.35, Ca^{2+} 0.4	• Best results: TTA•TOPO Single extraction Li^+ > 90%. • In pairs with Li^+; Li^+ ~ 80%(Na^+), Li^+ > 90 %(K^+), Li^+ ~ 10% (Mg^{2+}), Li^+ > 70 %(Ca^{2+})	[62]

applicability of these compounds is showcased in Table 1. Fig. 2 shows the structure of the extractants selected in this study.

3.1. Study of the nature of cation-ligand bond

The nature of the cation-extractant bond in these systems is a subject of wide speculation throughout the available literature [26]. Models based on dative bonds, free electron pairs or the hybridization of atomic orbitals in the $-C=O \bullet A^{m+}/-P=O \bullet A^{m+}$ ($-C=O$=carbonyl, $-P=O$=phosphate) systems are usually suggested in order to explain this bond, implying restrictions in the coordination of the cation. It is sometimes forgotten that these kinds of models are but a first approximation, and their validity becomes questionable under increasing system complexity. Furthermore, the cations under study already have a closed-shell structure, they are included within the group of hard acids, and therefore any hybridization with the oxygen p-orbitals is highly unlikely. This fact points towards a purely electrostatic attraction between the cation and the extractant with hardly any charge transfer towards the cation, as expected from hard metal ions following Pearson's principle [68]. This can be readily seen by looking at the electronic density of the systems at hand. The electronic density is directly related to the square of the electronic wave function -this is, in fact, the basis of

DFT-, and basically represents the location of the electrons in the atomic structure. Hence, a covalent bond -i.e. two atoms sharing electrons- would translate to a noticeable electronic density in the region between said atoms. In Fig. 3 it can be shown several representations of the normalized electronic density - meaning a volume integral over the whole molecule would yield N, the number of electrons. In Fig. 3a one can see a projection of the electronic density on the molecular plane of the Li$^+$•DBM system, taking advantage of its planar geometry. As expected, the electronic density accumulates around the nuclei and connects the atoms within the molecule. It is clear, too, that the electron density goes to zero in the bonding region, hence confirming the hypothesis that it is indeed an electrostatic (ionic) interaction. Similarly, Fig. 3b and Fig. 3c present (relatively low) electronic density isosurfaces of the Li$^+$•TOPO and Li(H$_2$O)$_4^+$ systems, where one can also observe how the electron clouds of the cation and the extractant(s) are clearly disconnected. Isosurface level in (b) and (c) was set to 0.08 [59,69].

Additionally, as previously described in Section 2.3, by analysing the topology of the electronic density one may partition it into basins corresponding to each of the atoms, effectively assigning them a charge. These processes further confirmed proposed claims, as only a slight charge transfer from the cations to the extractants of around ~0.1 a.u. (Group I) or ~0.3 a.u. (Group II) takes place throughout the considered
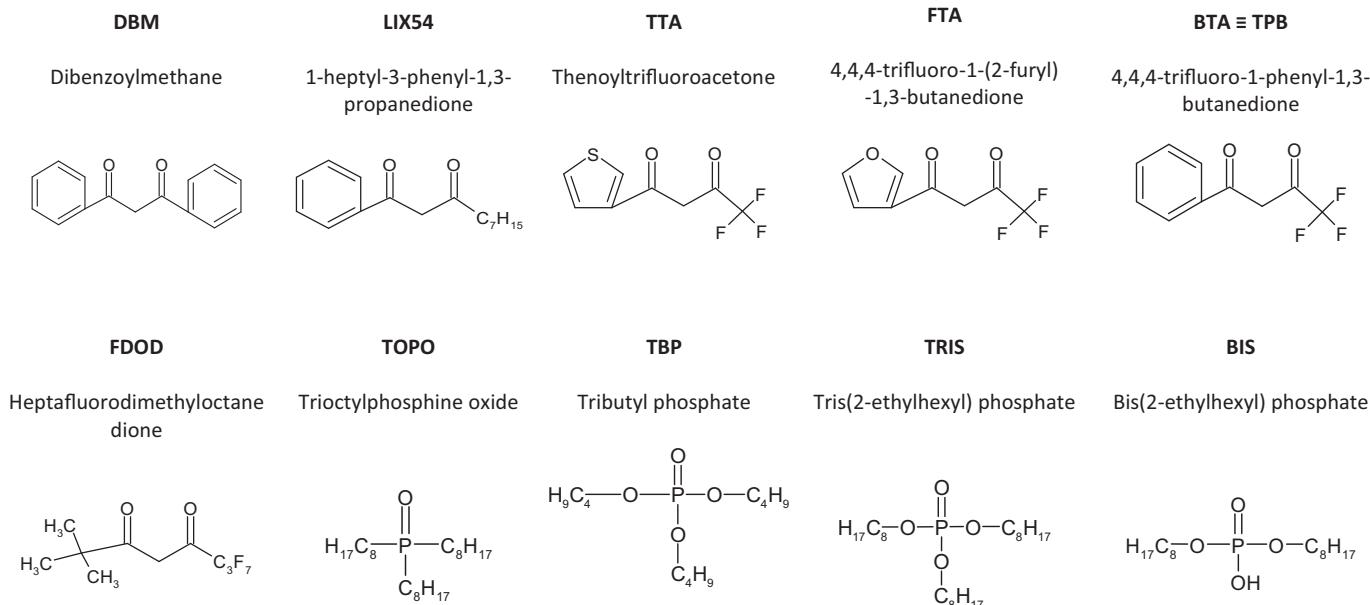
Fig. 2. Structural schematics of the extractants included in Table 1.
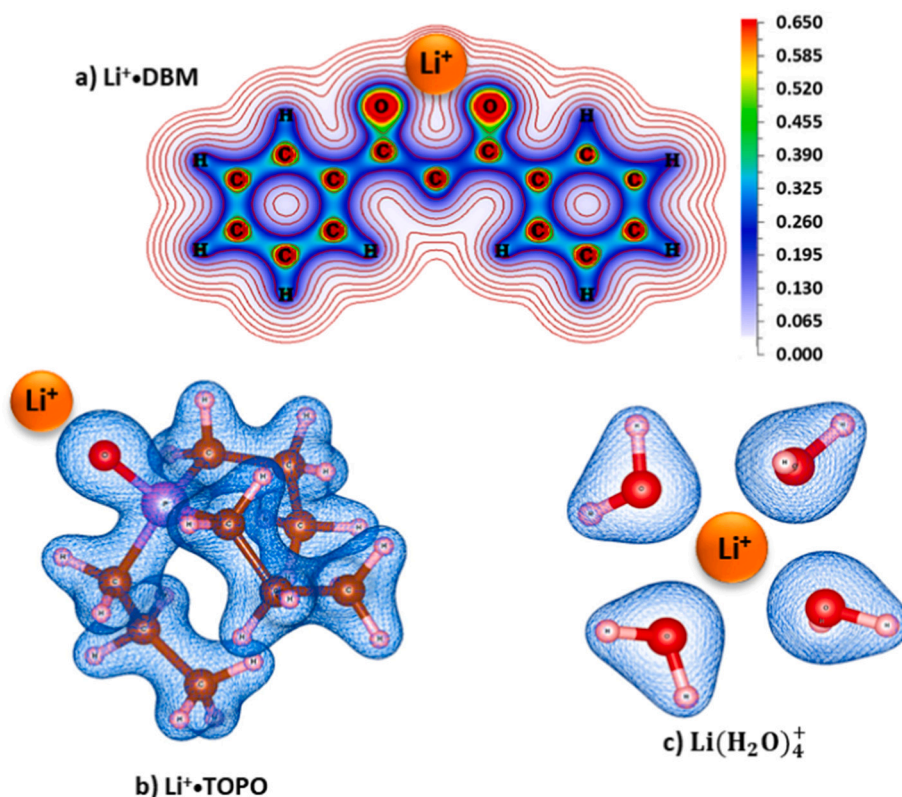
Fig. 3. Graphical representations of the normalized electronic density of lithium complexes with an β-diketone (a), with an organophosphate (b) and its hydration-shell (c).

systems. This ionic interaction appears to have a highly localized character too. Dramatic modifications on the extractants have a relatively low impact on binding energies, as evidenced by our initial exploration of different TOPO chain lengths (Fig. 1). This situation renders the double-bond oxygen atoms in the extractant molecules as the most likely docking location for the cations, as their high electronegativity drags the molecular electron cloud towards their general vicinity, providing a negatively charged region for the cations to bond. The implicit assumption in this model is that the concentration of cations is low enough so that each extractant molecule/complex will react with only one cation. During the simulation, it was found that association with more than one cation was unfavorable given that a single site of this kind exists per extractant. Thus, the model clearly contains approximations that can be valid over a large range of concentrations.

3.2. Geometric structures of extractant and complexes metal ionic • extractant

The cation-oxygen distances, i.e. those involving only the cation and a single extractant, either a β-diketone or an organophosphate-, seem to be the parameters more closely related to the strength of the bond. In Table 2 are collected these values of all the simple complexation reactions. In the case of the β-diketones two values are given, one for each oxygen, alongside their difference.

All distances lie in the 1.83 Å (Li$^+$) to 2.76 Å (K$^+$) range in the case of the β-diketones and between 1.68 Å (Li$^+$) and 2.45 Å (K$^+$) in the case of the phosphates, always ordered Li$^+$ < Mg^{2+} < Ca^{2+} < Na$^+$ < Sr^{2+} < K$^+$. This result is expected; it is mainly related to the size of the ions, the smaller the size, the shorter the distance between atoms (cation and oxygen) that is, greater electrostatic attraction and fewer electrostatic impediments. In the case of the elements of the same period, two cations, such as Na$^+$ and Mg^{2+}, have the same number of electrons with a different nuclear charge, hence group II cations will be smaller, due to

the larger core attraction, than the equivalent from group I. Conversely, in a group the size increases with the atomic number mainly as a consequence of the electrons of the last valence shell being at energy levels further away from the nucleus ($2s^1$ Li$^+$; $3s^1$ Na$^+$; $4s^1$ K$^+$). In the case of calcium and magnesium ions, the period and group effects cause both ions to show similar distances. β-Diketones also seem to have larger bonding distances compared to the organophosphates, most likely due to the competing attraction of the charge difference in both types of extractants. For example, the average charge of the Li$^+$•DBM oxygens is −1.24 a.u., whereas the Li$^+$•TOPO oxygen presents a charge of −1.6 a.u., most likely due to positively charged phosphorus atom (2.782 a.u) in the latter acting as an electron acceptor.

Despite the fact that all cations maintain a similar bond length no matter the choice of extractant, some slight trends may be observed: first, DBM complexes consistently bind closer than the rest ones for the same cationic species in the case of the β-diketones, and a similar thing happens between TOPO and the other phosphates as well. Secondly, there are some small differences (<0.1 Å) between the bond lengths of oxygen atoms of most β-diketones, most likely caused by the asymmetry of their radicals. This is evidenced by the fact that DBM complexes, where both distances are equivalent, are also the only ones with a 2-fold rotational axis (symmetry group C$_{2v}$). These differences are also systematically larger in the group II cations, suggesting unequal electrostatic interaction with the oxygen atoms. This theory may find support in the fact that LIX54 complexes, the only ones beside DBM ones with no highly electronegative atoms -such as fluorine- in its radicals, present the smallest deviations. In fact, if one looks at the charge of the oxygen atoms in the Li$^+$•FDOD and Li$^+$•TTA systems, the oxygen atoms closer to the fluorine radicals have a greater charge (−1.182 a.u. and −1.177 a.u. respectively) than the other one (−1.233 a.u. in both cases). The oxygen atoms in the Li$^+$•DBM and Li$^+$•LIX54 systems, on the other hand, have the same atomic charge (−1.24 a.u. in both cases). This negative charge reduction leads to an unequal attraction between the positively charged

Table 2
Distance (in Å) between the cations and the closest oxygen atom(s).

		Li$^+$		Na$^+$		K$^+$		Mg^{2+}		Ca^{2+}		Sr^{2+}	
β-diketones	DBM*	1.85	0.00	2.22	0.00	2.58	0.01	1.91	0.00	2.17	0.00	2.33	0.00
		1.85		2.22		2.59		1.91		2.17		2.33	
	DBM	1.83	0.00	2.20	0.00	2.59	0.01	1.91	0.00	2.16	0.00	2.33	0.00
		1.83		2.20		2.58		1.91		2.16		2.33	
	LIX54	1.86	0.02	2.25	0.02	2.65	0.03	1.92	0.03	2.20	0.05	2.38	0.05
		1.84		2.22		2.62		1.89		2.16		2.33	
	TTA	1.92	0.08	2.31	0.09	2.72	0.10	1.96	0.09	2.27	0.13	2.44	0.13
		1.83		2.21		2.62		1.88		2.14		2.31	
	FTA	1.91	0.08	2.28	0.08	2.70	0.12	1.98	0.09	2.27	0.14	2.47	0.16
		1.83		2.19		2.58		1.88		2.13		2.31	
	BTA	1.90	0.07	2.26	0.08	2.69	0.07	1.96	0.08	2.26	0.12	2.44	0.12
		1.83		2.18		2.63		1.88		2.15		2.32	
	FDOD	1.91	0.05	2.27	0.03	2.76	0.08	1.96	0.04	2.27	0.08	2.45	0.08
		1.87		2.24		2.69		1.91		2.18		2.36	
Organophosphates	TOPO	1.68		2.05		2.39		1.79		2.02		2.18	
	TBP	1.71		2.08		2.44		1.76		2.05		2.22	
	TRIS	1.71		2.07		2.43		1.80		2.00		2.21	
	BIS	1.71		2.09		2.45		1.81		2.06		2.22	

The MP2 results for DBM (DBM*) present a slightly weaker bond (~10 kcal/mol less) compared to DFT results, but seeing as this affects all cations equally, it may consider that the choice of the selected functional is valid.

cation and each of the oxygen, which together with the size and charge of the ions causes the observed discrepancies in the bond lengths.

Additionally, the structures of the β-diketones present deformations in their central C–C–C dihedral angles, i.e. the one formed by the carbons connecting the two main oxygen atoms, most likely due to the oxygen-oxygen repulsion. These stabilize when a cation is got into, as shown in Fig. 4, which may introduce a size-selectivity factor, similarly, to how crown-ether extractants are thought to discriminate between cations based on their cavity size [30,47,68]. For example, looking at the DBM case, the dihedral goes from 105° when no cation is present to <5° when complexed with Li$^+$.

3.3. Thermochemistry study

This section presents the results of the thermodynamic study of the simple and mixtures of extractants in order to obtain reaction energy (ΔE), free energy (ΔG), extraction constant K and selectivity of lithium.

3.3.1. Cation ● β-diketone and cation ● organophosphate complexes

The ΔE and ΔG changes for said reactions were obtained using the ORCA 4.2.1 quantum chemistry package [57,58] at the B3LYP/def2-SVP level of theory (Section 2.3). These results are graphed in Fig. 5, together alongside the same energies for the hydration reaction of the cations.

All reactions display negative ΔE and ΔG values, meaning the final complexes are stable and that the reaction may happen spontaneously. The geometry optimization of the molecules (products and reactants) was minimized by numerical methods, such as conjugated gradient descent (CGD) (Section 2.1). The thermal contribution of the entropy to ΔG was found to be similar ($TS \sim -10$ kcal/mol) throughout all systems.

In a complexation reaction, one may always expect a negative entropy change due to the reduction in the number of molecules in the system, and hence similar values arise from the fact that all reactions share the same stoichiometry. The MP2 results for DBM (DBM*) present a slightly weaker bond (~10 kcal/mol less) compared to DFT results, but seeing as this affects all cations equally, it may consider that the choice of the selected functional is valid.

In general terms, bonds with group II cations are consistently stronger compared to those in group I, reinforcing the idea that the bond is electrostatic in nature; the bond strength decreases with increasing cation size, and therefore increasing bonding distance. This is again to be expected, as the inverse relationship between cation size and electronegativity should weaken the electrostatic bond. For example, the K$^+$ bonds usually lie in the −25 kcal/mol region, roughly half as strong as the Li$^+$ one. The most bonding group I cation is always Li$^+$, with around −50 to −40 kcal/mol, compared to the −120 to −90 kcal/mol from the Mg^{2+} cation of group II (Fig. 5a).

Due to the smaller bond lengths in DBM and LIX54 complexes (Table 2), the cations bind to these extractants more strongly than to the rest (less ΔG greater K_{ec} (Eq. (5))). Again, this might be explained by the absence of fluorine atoms in their radicals, whose electrophilic character draws the electronic density away from the oxygen region and hence weaken the cation-extractant electrostatic interaction. This would also explain why TOPO complexes bond more strongly than the other phosphates, as the latter has additional oxygen atoms before the carbon chains that cause a similar effect to the fluorine atoms in the β-diketones (Fig. 5b). For example, although there is not much difference, in the case of Li$^+$ ΔG has a value around −43 kcal/mol for Li$^+$●DBM and Li$^+$●LIX54, lower (absolute value) for the rest of the extractants, with the exception
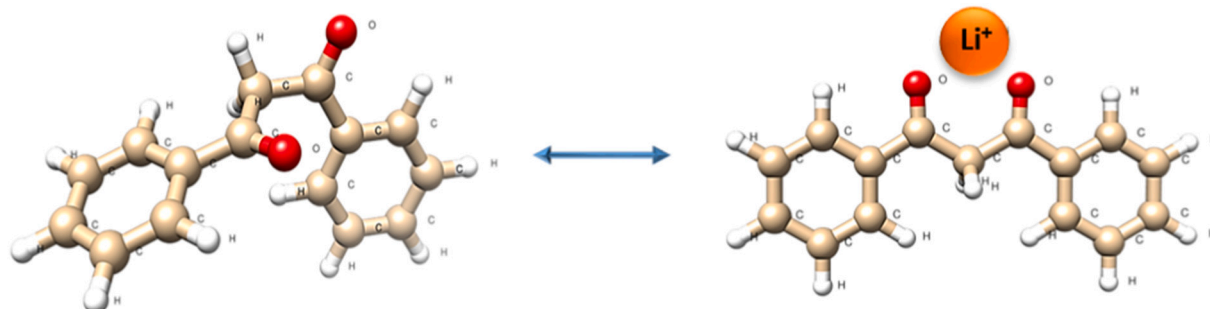
Fig. 4. Graphical representation of the structural changes of the DBM β-diketone during the complexation reaction with a Li$^+$ cation [70].
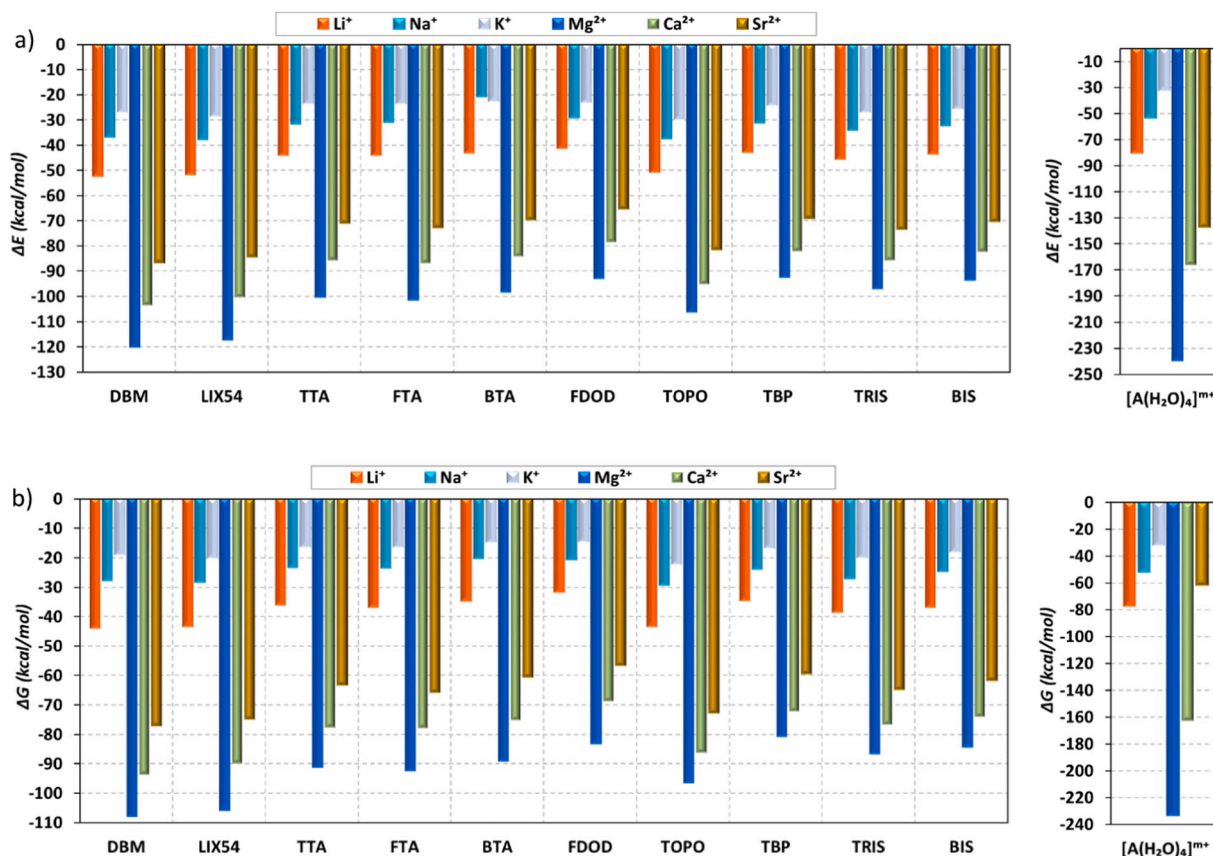
Fig. 5. Changes in reaction ΔE (a) and free energy ΔG (b) of the cation ● extractant (β-diketone or phosphate) complexation reactions.

of TOPO. In general terms, the complexes will be formed follow the order $Mg^{2+} > Ca^{2+} > Sr^{2+} > Li^{+} > Na^{+} > K^{+}$ and preferably with β-diketones.

Finally, looking at Fig. 5 it is also clear that the cations bond far more strongly with the water shell bonds than any of the extractants, especially the cations of group II due to their smaller size. This makes sense, seeing as the water molecules are basically four oxygen atoms that surround the cation in an efficient, tetragonal structure.

3.3.2. Cation ● β-diketone ● organophosphate complexes

As previously mentioned in Section 1, β-diketones and phosphates (mainly TOPO) commonly are used together in the laboratory, as a synergistic effect has been observed lithium extraction is greatly improved when both extractants are combined (compound complexes). Based on the energy results of the simple systems shown in Section 3.3.1 organophosphate TOPO was selected in order to study the synergic effect of β-diketone ● organophosphate extractants on the extraction of Li^{+} in the presence of Na^{+}, K^{+}, Mg^{2+}, Ca^{2+} and Sr^{2+} from seawater desalination concentrates. Fig. 6 shows ΔE and ΔG for the cation ● β-diketone ● TOPO complexation reactions.

As it can be observed in Fig. 6a, the hypothesis regarding the synergic effect of extractants was confirmed by simulations reached in this work; general way, combining the β-diketones with TOPO in a 1:1, ratio strengthened the reaction energy increase up (absolute value) from 56.8% for Ca²⁺●DBM●TOPO complex to 207% for Na⁺●BTA●TOPO complex versus simples complexes. This, however, is no longer the case when a second TOPO is added to the reaction, as through trial simulations we found this reaction mechanism to yield a far less energetically favourable reaction product, to the point where the reaction is non-spontaneous ($\Delta G > 0$) for group I cations and far less favourable than the 1:1 stoichiometry for group II ones, contrary bibliographic claims [71]. This scenario can be due to steric issues, as the interaction of the

TOPO chains with the β-diketone radicals appears to hinder -or at least compete with- the coordination of the phosphate's oxygen atoms around the cation (see Fig. 7). It must be noted that all Li^{+} systems, both with water and extractants alike, have a bonding free energy of approximately -20 kcal/mol per oxygen atom surrounding the cation. Hence it seems reasonable to suspect that the β-diketones and the TOPO replace three of the water molecules in the cation's hydration shell, possibly leaving one still attached to the cation.

Regarding ΔG, the largest differences between simple and complex systems are for the systems $(Li^{+}; Mg^{2+}; Ca^{2+}; Sr^{2+})$●FDOD●TOPO (around 110%) and $(Na^{+}; K^{+})$●BTA●TOPO (between 120 and 200%). Based on the free energy, the extraction order of the cations is $Mg^{2+} > Ca^{2+} > Sr^{2+} > Li^{+} > Na^{+} > K^{+}$, Mg^{2+}, Ca^{2+} and Sr^{2+} cations have slightly higher free energy, between 1.8 (Sr^{2+}) to 2.6 (Mg^{2+}) times, than lithium with DBM●TOPO and LIX54●TOPO systems (Fig. 8). In this sense, it can be thought that lithium could not be selectively extracted against these cations, however, the hydration energy of these cations must be taken into account, since it shows how energetically the cations are bound to the water molecules. Thus, the analysis of the relation of the equilibrium constants of the complexation (k_{ec}) and hydration (k_{eh}) reactions is carried out in the next section, in order to analyse selective extraction of lithium from seawater desalination concentrates.

3.3.3. Equilibrium constants and selectivity lithium from seawater desalination concentrates

Using the free energy ΔG obtained in Section 3.3.2 and employing Eq. (5) it has been computed complexation (k_{ec}) and hydration (k_{eh}) reactions for each cation. These constants were subsequently used to calculate the extraction constant K (Eq. (8)). The natural logarithm of the extraction constant for each combination cation ● extractant/s is represented in Fig. 9. Numerical values of the natural logarithm of k_{ec}, k_{eh} and K are available in the supplementary material.
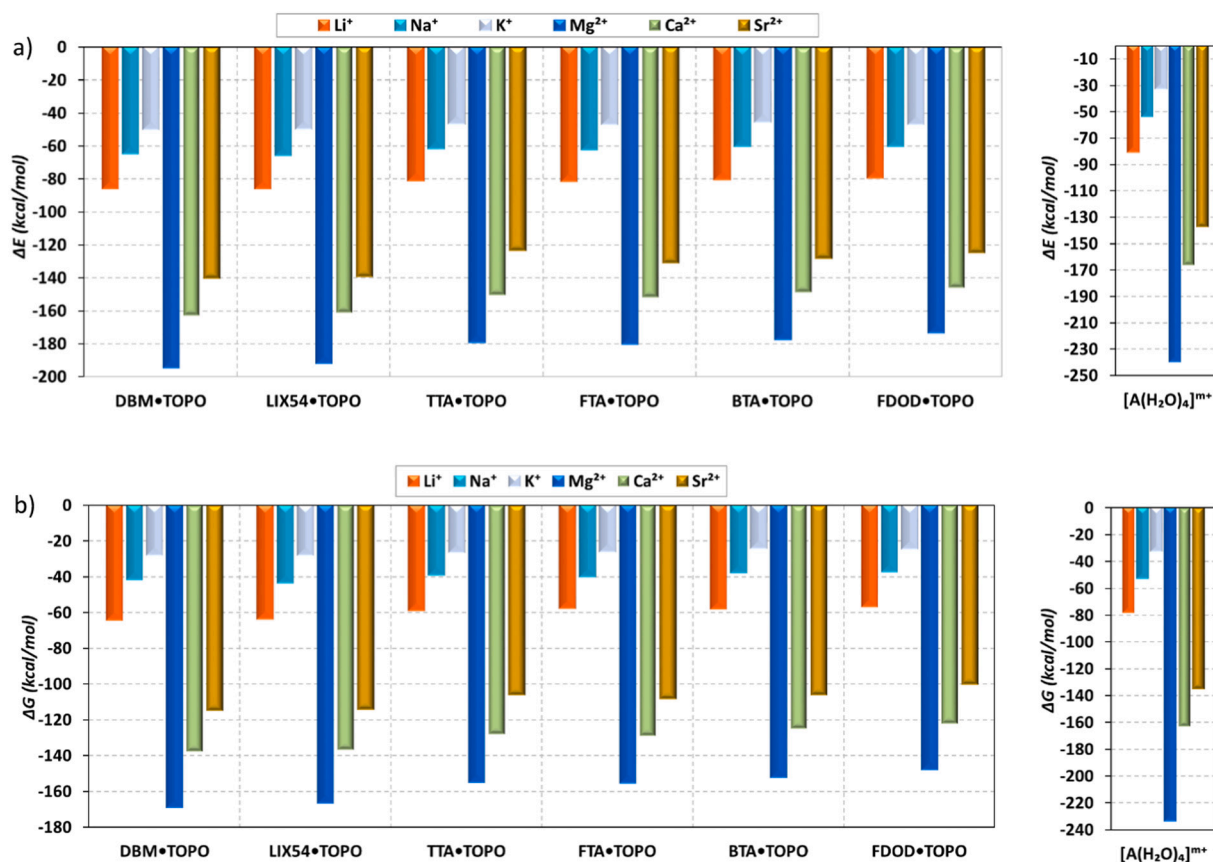
Fig. 6. Changes in reaction ΔE (a) and free energy ΔG (b) during the cation • β-diketone • TOPO complexation reactions.
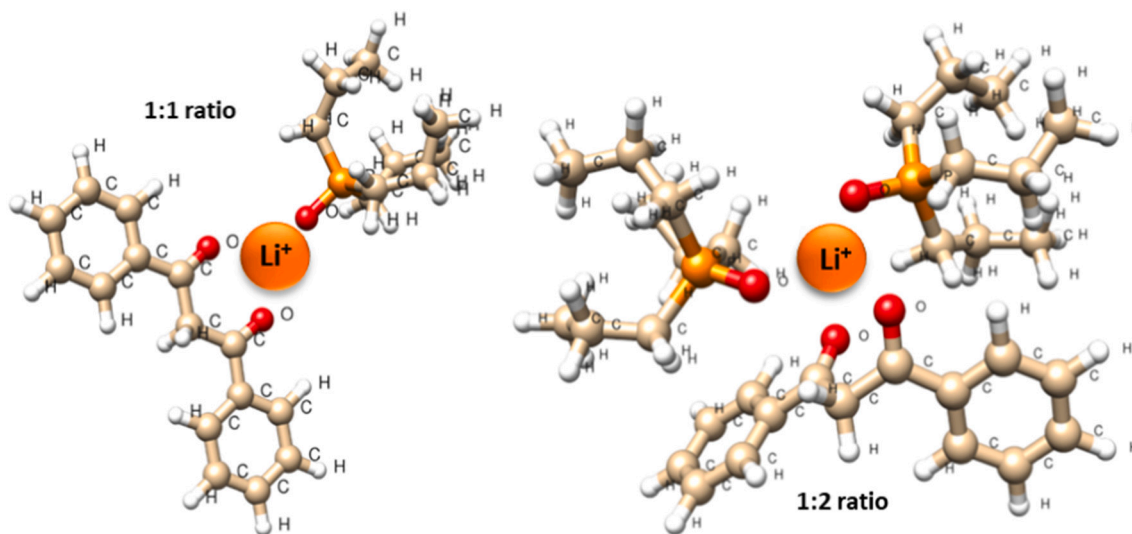
Fig. 7. Alternative stoichiometries of Li$^+$•DBM•TOPO complexation.

As expected, the extraction constant directly correlates with the ΔG results: composite systems perform better (have a more positive ln(K)) than simple ones. The extraction coefficients for all cations are major when the combined extractant systems are used than in the case of using a single extractant. Additionally, all group I cations have a better extraction constant K compared to group II ones so much each extractant and each extractants combination following the order $K(K^+) > K(Na^+) > K(Li^+) > K(Sr^{2+}) > K(Ca^{2+}) > K(Mg^{2+})$ (Fig. 9). This may seem striking at first, considering how the bonds of the latter are generally

stronger than those of the former, but one must also bear in mind that group II cations sport much larger hydration constant (k_{eh}), and hence, are harder to extract of aqueous phase than cations of group I ($lnk_{eh} = 394.20$ (Mg^{2+}) $> lnk_{eh} = 274.99$ (Ca^{2+}) $> lnk_{eh} = 227.15$ (Sr^{2+}) $> lnk_{eh} = 131.21$ (Li$^+$) $> lnk_{eh} = 88.27$ (Na$^+$) $> lnk_{eh} = 53.94$ (K$^+$)). As previously mentioned in Section 2.2, the choice of $n = 4$ as coordination number was made somewhat arbitrarily in order to compare all cations equally. While this choice is appropriate for Li$^+$ (and also Mg^{2+}, due to their similar ionic size), it is thought that the appropriate coordination
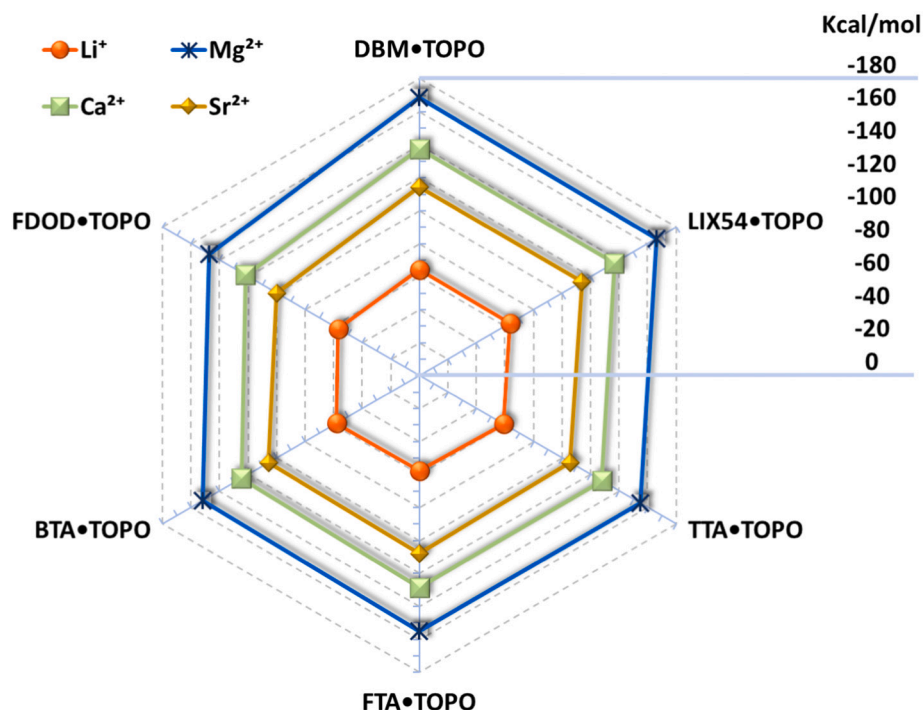
Fig. 8. Changes free energy, ΔG, during the (Mg^{2+}; Ca^{2+}; Sr^{2+}; Li^+) • β-diketone • TOPO complexation reactions.

number for the larger cations is also higher ($n = 5$ for Na^+, $n = 6$ for K^+, $n = 8$ for Ca^{2+}, etc. [46,72]). This means that Na^+ and K^+ hydration energies are probably underestimated, as there should be more water molecules in their hydration shell, hence augmenting their k_{eh}. This means, however, that even in the worst case scenario for lithium, it is still selectively extracted over all group II cations [31], and to a lower extent from other cations from group I.

Once extraction constant K has been calculated for all systems, it is of special interest to determine the selectivity of Li^+ regarding the rest of the metal ions presenting seawater desalination concentrates. Fig. 10a shows the lithium selectivity for group II cations and extractant or extractants combined, calculated as defined in Section 2.2 (Eq. (9)). In the same way, Fig. 10b shows the lithium selectivity for group I cations and extractant or extractants combined. In addition, Fig. 10b shows the

selectivity of Li^+ regarding the rest of the cations.

First of all, it should be noted that the selectivity values give a qualitative character to the separation reached in this study, since it is a quotient of very small equilibrium constants. As it is expected, based on extraction constant K, Li^+ is selective towards group II metal ion (Fig. 10a). The order of selectivity is S(Li^+/Mg^{2+}) > S(Li^+/Ca^{2+}) > S (Li^+/Sr^{2+}). The highest selectivity is referred to TBP, TRIS and BIS extractants system and for the combined mixtures BTA•TOPO and FDOD•TOPO. However, following equal reasoning, Fig. 10b shows that Li^+ is less selective towards the group I metal ions, being S(Li^+/Na^+) > S (Li^+/K^+). In this situation, β-diketone extractants, DBM and LIX54 are the most selective in individual simulations, but mixtures are more selective, with DBM•TOPO coming first, followed by LIX54•TOPO and BTA•TOPO. Contrary to the case of group II, FDOD•TOPO is least selective.

Finally, it can be concluded that selectivity of Li^+ regarding the rest of the cations and the 16 extractants and mixtures of extractants studied (Fig. 10b), i) is lower than the selectivity with respect to each cation, and approximately equal to selectivity Li^+/K^+ due to the fact that the K of potassium is significantly lower than that of the rest, ii) the most selective extractants are FDOD•TOPO for group II metal ions and DBM•TOPO for group I. It is worth noting that in correspondence with the extraction constants, the DBM•TOPO mixture is the one with the highest extraction constant value. In view of the results obtained, the decision to use one or another extractant or their combination will depend on the needs raised, as well as the possibility of developing an extraction process in stages.

4. Conclusions

In this work, a computational study of the most promising of extractants towards lithium in presence of the metal ions found in higher concentrations in the desalination brines such as Na^+, K^+, Mg^{2+}, Ca^{2+} and Sr^{2+} was carried out. For this, their equilibrium and thermodynamic properties have been obtained via molecular simulation using ab initio Density Functional Theory (DFT) simulations.

To the best of knowledge, it was managed to clarify the nature and
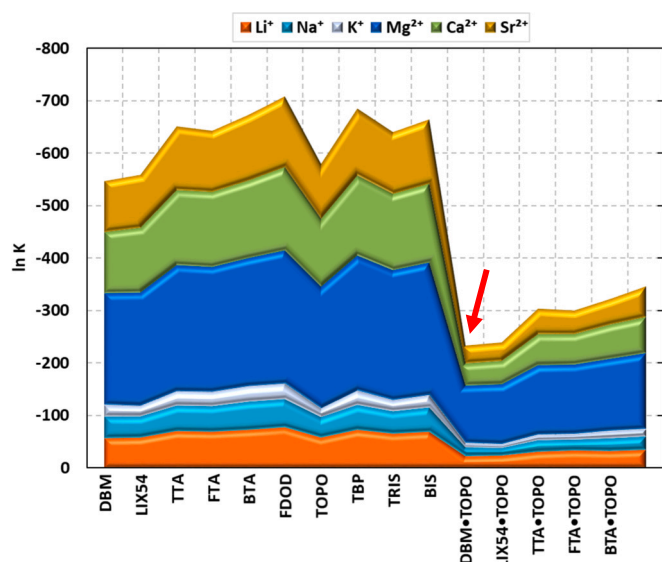
Fig. 9. ln$K$ for cation • extractant/s systems.
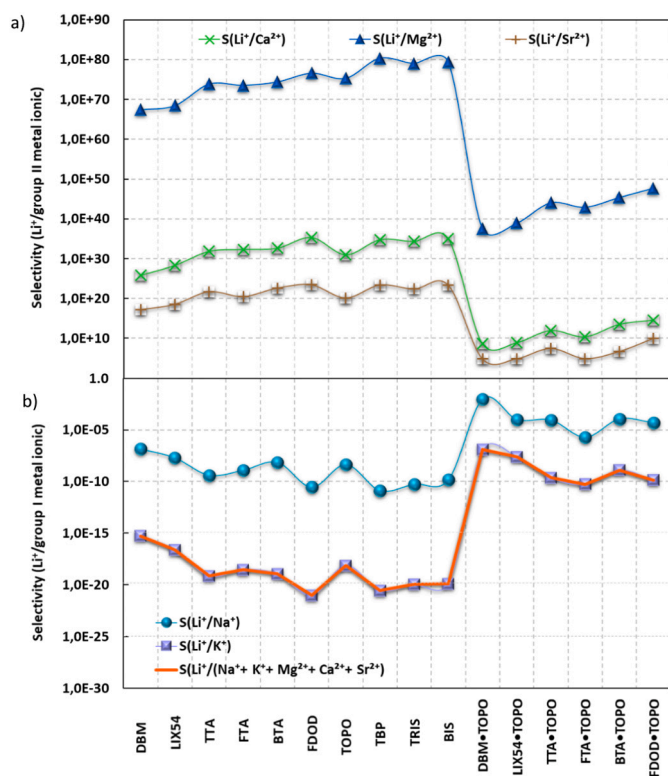
Fig. 10. a) Li$^+$ selectivity for group II cations and extractant or extractants combined, b) Li$^+$ selectivity for group I cations and extractant or extractants combined and selectivity of Li$^+$ regarding the rest of the cations.

distance of cation-extractant/s bonding for the first time in the open literature. Using the square of the electronic wave function it was observed that the electronic density accumulates around the nuclei and connects the atoms within the molecule going to zero in the bonding region, confirming that it is an electrostatic (ionic) interaction. The double-bond oxygen atoms in the β-diketones are the most likely docking location for the cations. Regarding the bond distance, both in the case of the β-diketones and phosphates, Li$^+$ presented the shortest distance versus the rest of the cations, especially with the extractants DBM and TOPO. By and large, β-diketones showed larger bonding distances compared to the organophosphates. The presence of highly electronegative species in the radicals of the extractants, such as fluorine (β-diketones) or additional oxygen atoms (organophosphates), appears to weaken the cation-ligand bond.

The complexation reaction energies of the simple systems formed by a cation and a single extractant (β-diketone or organophosphate) displayed negative ΔE and ΔG values, meaning the final complexes are stable and that the reaction may happen spontaneously. In general terms, the complexes were formed follow the order Mg^{2+} > Ca^{2+} > Sr^{2+} > Li$^+$ > Na$^+$ > K$^+$ and preferably with β-diketones, especially DBM and LIX54 and organophosphate TOPO. Base on the energy results of the simple systems, organophosphate TOPO was selected in order to study the synergic effect of β-diketone • organophosphate extractants on the extraction of Li$^+$. Combining the β-diketones with TOPO in a 1:1 ratio increased the reaction energy and the free energy (absolute value) versus simples systems (keeping the order of extraction). Based on the ΔG, the best extraction was for the cations Mg^{2+} > Ca^{2+} > Sr^{2+} > Li$^+$ > Na$^+$ > K$^+$ and the DBM•TOPO and LIX54•TOPO systems.

With the aim of studying the selective extraction of lithium, the analysis of the relation of the equilibrium constants of complexation (k_{ec}) and the constants of hydration of the cations (k_{eh}) named extraction coefficient, K. This coefficient followed the order K(K$^+$) > K(Na$^+$) > K(Li$^+$) > K(Sr^{2+}) > K(Ca^{2+}) > K(Mg^{2+}) due to mainly that group II cations

sport much larger hydration constant. K(Li$^+$) could get better due to Ca^{2+}, Sr^{2+}, Na$^+$ and K$^+$ hydration energies are probably underestimated, as there should be more water molecules in their hydration shell, hence augmenting their k_{eh}. Coordination number $n = 4$ was used arbitrarily to calculate simulation. Finally, selectivity Li$^+$ towards each cation and selectivity towards total cations was calculated. The order of selectivity regarding cations of the group II was S(Li$^+$/Mg^{2+}) > S(Li$^+$/Ca^{2+}) > S(Li$^+$/Sr^{2+}) referred to TBP, TRIS and BIS extractants system and for the combined mixtures BTA•TOPO and FDOD•TOPO. Li$^+$ cation was less selective towards the group I metal ions, being S(Li$^+$/Na$^+$) > S(Li$^+$/K$^+$) for β-diketone extractants, DBM and LIX54 and DBM•TOPO, LIX54•TOPO and BTA•TOPO. Selectivity of Li$^+$ regarding the rest of the cations and the 16 extractants and mixtures of extractants studied was lower than the selectivity of Li$^+$ with respect to each individual cation and similar to S(Li$^+$/K$^+$).

It is expected that the results obtained from these simulations will contribute to a better understanding how these extractants act with regard to the selective extraction of Li$^+$ in seawater desalination concentrates, and, therefore, reduce the experimental work required in these studies. In view of the results obtained in this work, the decision to use one or the other extractant or its combination will depend on the needs raised, as well as the possibility of developing an extraction process in stages.

Supplementary data to this article can be found online at https://doi.org/10.1016/j.desal.2022.115704.

CRediT authorship contribution statement

R. Coterillo: Conceptualization, Methodology, Software, Writing-Original Draft. **L.-E. Gallart:** Investigation, Formal analysis, Writing-Original Draft. **E. Fernández-Escalante:** Investigation, Formal analysis, Writing-Original Draft. **J. Junquera:** Conceptualization, Methodology, Software. **P. García-Fernández:** Conceptualization, Methodology, Software. **I. Ortiz:** Resources. **R. Ibañez:** Conceptualization, Investigation, Resources, Funding acquisition. **M.-F. San-Román:** Conceptualization, Formal analysis, Writing - Review & Editing, Supervision, Funding acquisition.

Declaration of competing interest

The authors declare that they have no known competing financial interests or personal relationships that could have appeared to influence the work reported in this paper.

Acknowledgements

References

[1] P. Xu, J. Hong, X. Qian, Z. Xu, H. Xia, X. Tao, Z. Xu, Q.Q. Ni, Materials for lithium recovery from salt lake brine, J. Mater. Sci. 56 (2021) 16–63, https://doi.org/10.1007/s10853-020-05019-1.

[2] U.S. Geological Survey, Mineral Commodity Summaries 2021, 2021, https://doi.org/10.3133/mcs2021.

[3] U.S. Geological Survey, Mineral Commodity Summaries 2020, 2020. https://pubs.usgs.gov/periodicals/mcs2020/mcs2020.pdf.

[4] B. Swain, Recovery and recycling of lithium: a review, Sep. Purif. Technol. 172 (2017) 388–403, https://doi.org/10.1016/j.seppur.2016.08.031.

[5] Y. Sun, Q. Wang, Y. Wang, R. Yun, X. Xiang, Recent advances in magnesium/lithium separation and lithium extraction technologies from salt lake brine, Sep. Purif. Technol. 256 (2021), 117807, https://doi.org/10.1016/j.seppur.2020.117807.

[6] V. Flexer, C.F. Baspineiro, C.I. Galli, Lithium recovery from brines: a vital raw material for green energies with a potential environmental impact in its mining and

processing, Sci. Total Environ. 639 (2018) 1188–1204, https://doi.org/10.1016/j.scitotenv.2018.05.223.

[7] F. Arroyo, J. Morillo, J. Usero, D. Rosado, H. el Bakouri, Lithium recovery from desalination brines using specific ion-exchange resins, Desalination 468 (2019), 114073, https://doi.org/10.1016/j.desal.2019.114073.

[8] H. Joo, S. Kim, S. Kim, M. Choi, S.H. Kim, J. Yoon, Pilot-scale demonstration of an electrochemical system for lithium recovery from the desalination concentrate, Environ. Sci.: Water Res. Technol. 6 (2020) 290–295, https://doi.org/10.1039/c9ew00756c.

[9] S. Kim, H. Joo, T. Moon, S.H. Kim, J. Yoon, Rapid and selective lithium recovery from desalination brine using an electrochemical system, Environ. Sci.: Processes Impacts 21 (2019) 667–676, https://doi.org/10.1039/c8em00498f.

[10] E. Jones, M. Qadir, M.T.H. van Vliet, V. Smakhtin, S.Mu Kang, The state of desalination and brine production: a global outlook, Sci. Total Environ. 657 (2019) 1343–1356, https://doi.org/10.1016/j.scitotenv.2018.12.076.

[11] C. Xiao, L. Zeng, Thermodynamic study on recovery of lithium using phosphate precipitation method, Hydrometallurgy 178 (2018) 283–286, https://doi.org/10.1016/j.hydromet.2018.05.001.

[12] X. Lai, P. Xiong, H. Zhong, Extraction of lithium from brines with high Mg/Li ratio by the crystallization-precipitation method, Hydrometallurgy 192 (2020) 105252, https://doi.org/10.1016/j.hydromet.2020.105252.

[13] S. Wei, Y. Wei, T. Chen, C. Liu, Y. Tang, Porous lithium ion sieves nanofibers: general synthesis strategy and highly selective recovery of lithium from brine water, Chem. Eng. J. 379 (2020), 122407, https://doi.org/10.1016/j.cej.2019.122407.

[14] D. Gu, W. Sun, G. Han, Q. Cui, H. Wang, Lithium ion sieve synthesized via an improved solid state method and adsorption performance for west Taijinar salt Lake brine, Chem. Eng. J. 350 (2018) 474–483, https://doi.org/10.1016/j.cej.2018.05.191.

[15] S.H. Park, J.H. Kim, S.J. Moon, J.T. Jung, H.H. Wang, A. Ali, C.A. Quist-Jensen, F. Macedonio, E. Drioli, Y.M. Lee, Lithium recovery from artificial brine using energy-efficient membrane distillation and nanofiltration, J. Membr. Sci. 598 (2020), 117683, https://doi.org/10.1016/j.memsci.2019.117683.

[16] Y. Li, Y.J. Zhao, H. Wang, M. Wang, The application of nanofiltration membrane for recovering lithium from salt lake brine, Desalination 468 (2019), 114081, https://doi.org/10.1016/j.desal.2019.114081.

[17] B.K. Pramanik, M.B. Asif, S. Kentish, L.D. Nghiem, F.I. Hai, Lithium enrichment from a simulated salt lake brine using an integrated nanofiltration-membrane distillation process, J. Environ. Chem. Eng. 7 (2019), 103395, https://doi.org/10.1016/j.jece.2019.103395.

[18] S. Kim, J. Lee, J.S. Kang, K. Jo, S. Kim, Y.E. Sung, J. Yoon, Lithium recovery from brine using a λ-MnO$_2$/activated carbon hybrid supercapacitor system, Chemosphere 125 (2015) 50–56, https://doi.org/10.1016/J.chemosphere.2015.01.024.

[19] M.S. Palagonia, D. Brogioli, F. la Mantia, Lithium recovery from diluted brine by means of electrochemical ion exchange in a flow-through-electrodes cell, Desalination 475 (2020), 114192, https://doi.org/10.1016/J.desal.2019.114192.

[20] Z. Ren, X. Wei, R. Li, W. Wang, Y. Wang, Z. Zhou, Highly selective extraction of lithium ions from salt lake brines with sodium tetraphenylborate as co-extractant, Sep. Purif. Technol. 269 (2021), 118756, https://doi.org/10.1016/j.seppur.2021.118756.

[21] J. Li, H. Yi, M. Wang, F. Yan, Q. Zhu, S. Wang, J. Li, B. He, Z. Cui, Preparation of crown-ether-functionalized polysulfone membrane by in situ surface grafting for selective adsorption and separation of Li$^+$, ChemistrySelect 5 (2020) 3321–3329, https://doi.org/10.1002/slct.201904836.

[22] D. Shi, B. Cui, L. Li, M. Xu, Y. Zhang, X. Peng, L. Zhang, F. Song, L. Ji, Removal of calcium and magnesium from lithium concentrated solution by solvent extraction method using D2EHPA, Desalination 479 (2020), 114306, https://doi.org/10.1016/j.desal.2019.114306.

[23] R.E.C. Torrejos, G.M. Nisola, H.S. Song, L.A. Limjuco, C.P. Lawagon, K. J. Parohinog, S. Koo, J.W. Han, W.J. Chung, Design of lithium selective crown ethers: synthesis, extraction and theoretical binding studies, Chem. Eng. J. 326 (2017) 921–933, https://doi.org/10.1016/j.cej.2017.06.005.

[24] H. Su, Z. Li, Z. Zhu, L. Wang, T. Qi, Extraction relationship of Li$^+$ and H$^+$ using tributyl phosphate in the presence of Fe(III), Sep. Sci. Technol. 55 (2020) 1677–1685, https://doi.org/10.1080/01496395.2019.1604759.

[25] X. Zhang, W. Zhao, Y. Zhang, V. Jegatheesan, A review of resource recovery from seawater desalination brine, Rev. Environ. Sci. Biotechnol. 20 (2021) 333–361, https://doi.org/10.1007/s11157-021-09570-4.

[26] B. Swain, Separation and purification of lithium by solvent extraction and supported liquid membrane, analysis of their mechanism: a review, J. Chem. Technol. Biotechnol. 91 (2016) 2549–2562, https://doi.org/10.1002/jctb.4976.

[27] Z. Li, J. Mercken, X. Li, S. Riaño, K. Binnemans, Efficient and sustainable removal of magnesium from brines for lithium/magnesium separation using binary extractants, ACS Sustain. Chem. Eng. 7 (2019) 19225–19234, https://doi.org/10.1021/acssuschemeng.9b05436.

[28] S. Virolainen, M. Fallah Fini, V. Miettinen, A. Laitinen, M. Haapalainen, T. Sainio, Removal of calcium and magnesium from lithium brine concentrate via continuous counter-current solvent extraction, Hydrometallurgy 162 (2016) 9–15, https://doi.org/10.1016/j.hydromet.2016.02.010.

[29] S. Yang, G. Liu, J. Wang, L. Cui, Y. Chen, Recovery of lithium from alkaline brine by solvent extraction with functionalized ionic liquid, Fluid Phase Equilib. 493 (2019) 129–136, https://doi.org/10.1016/j.fluid.2019.04.015.

[30] K.S. Diao, H.J. Wang, Z.M. Qiu, A DFT study on the selective extraction of metallic ions by 12-crown-4, J. Solut. Chem. 38 (2009) 713–724, https://doi.org/10.1007/s10953-009-9406-3.

[31] T. Hanada, M. Goto, Synergistic deep eutectic solvents for lithium extraction, ACS Sustain. Chem. Eng. 9 (2021) 2152–2160, https://doi.org/10.1021/acssuschemeng.0c07606.

[32] B.I. El-Eswed, M. Sunjuk, R. Ghuneim, Y.S. Al-Degs, M.Al Rimawi, Y. Albawarshi, Competitive extraction of Li, Na, K, Mg and Ca ions from acidified aqueous solutions into chloroform layer containing diluted alkyl phosphates, J. Colloid Interface Sci. 587 (2021) 229–239, https://doi.org/10.1016/j.jcis.2020.12.029.

[33] Z. Zhou, J. Fan, X. Liu, Y. Hu, X. Wei, Y. Hu, W. Wang, Z. Ren, Recovery of lithium from salt-lake brines using solvent extraction with TBP as extractant and FeCl$_3$ as co-extraction agent, Hydrometallurgy 191 (2020), 105244, https://doi.org/10.1016/j.hydromet.2019.105244.

[34] S. Chen, X. Nan, N. Zhang, L. Li, X. Yu, Y. Guo, T. Deng, Solvent extraction process and extraction mechanism for lithium recovery from high Mg/Li-ratio brine, J. Chem. Eng. Jpn 52 (2019) 508–513, https://doi.org/10.1252/jcej.17we230.

[35] Z. Zhou, H. Liu, J. Fan, X. Liu, Y. Hu, Y. Hu, Y. Wang, Z. Ren, Selective extraction of lithium ion from aqueous solution with sodium phosphomolybdate as a coextraction agent, ACS Sustain. Chem. Eng. 7 (2019) 8885–8892, https://doi.org/10.1021/acssuschemeng.9b00898.

[36] W. Chen, X. Li, L. Chen, G. Zhou, Q. Lu, Y. Huang, Y. Chao, W. Zhu, Tailoring hydrophobic deep eutectic solvent for selective lithium recovery from the mother liquor of Li$_2$CO$_3$, Chem. Eng. J. (2021), 127648, https://doi.org/10.1016/j.cej.2020.127648.

[37] Y. Pranolo, Z. Zhu, C.Y. Cheng, Separation of lithium from sodium in chloride solutions using SSX systems with LIX 54 and Cyanex 923, Hydrometallurgy 154 (2015) 33–39, https://doi.org/10.1016/j.hydromet.2015.01.009.

[38] E.E. Çelebi, M.S. Öncel, M. Kobya, M. Bayramoğlu, Extraction of lithium from wastewaters using a synergistic solvent extraction system consisting of mextral EOL and Cyanex 923, Hydrometallurgy 185 (2019) 46–54, https://doi.org/10.1016/J.hydromet.2019.01.016.

[39] Y.Steven Kurniawan, R.Rao Sathuluri, K. Ohto, W. Iwasaki, H. Kawakita, S. Morisada, M. Miyazaki, Jumina, A rapid and efficient lithium-ion recovery from seawater with tripropyl-monoacetic acid calix[4]arene derivative employing droplet-based microreactor system, Sep. Sci. Technol. 211 (2019) 925–934, https://doi.org/10.1016/j.seppur.2018.10.049.

[40] S. Katsuta, H. Nomura, T. Egashira, N. Kanaya, Y. Kudo, Highly lithium-ion selective ionophores: macrocyclic trinuclear complexes of methoxy-substituted arene ruthenium bridged by 2,3-pyridinediolate, New J. Chem. 37 (2013) 3634–3639, https://doi.org/10.1039/c3nj00761h.

[41] L. Zhang, L. Li, D. Shi, X. Peng, F. Song, F. Nie, W. Han, Recovery of lithium from alkaline brine by solvent extraction with β-diketone, Hydrometallurgy 175 (2018) 35–42, https://doi.org/10.1016/j.hydromet.2017.10.029.

[42] P.Y. Ji, Z.Y. Ji, Q.B. Chen, J. Liu, Y.Y. Zhao, S.Z. Wang, F. Li, J.S. Yuan, Effect of coexisting ions on recovering lithium from high Mg^{2+}/Li$^+$ ratio brines by selective-electrodialysis, Sep. Purif. Technol. 207 (2018) 1–11, https://doi.org/10.1016/j.seppur.2018.06.012.

[43] Donald A. McQuarrie, Statistical Mechanics, University Science Books, 2000.

[44] S. Hammes-Schiffer, A conundrum for density functional theory: DFT studies may sometimes get the right results for the wrong reasons, Science 355 (2017) 28–29, https://doi.org/10.1126/science.aal3442.

[45] C.J. Cramer, Essentials of computational chemistry: theories and models, in: 2°, Wiley, 2004.

[46] S. Varma, S.B. Rempe, Coordination numbers of alkali metal ions in aqueous solutions, Biophys. Chem. 124 (2006) 192–199, https://doi.org/10.1016/j.bpc.2006.07.002.

[47] Y. Yao, M. Zhu, Z. Zhao, W. Liu, B. Tong, M. Li, Density functional theory study of selectivity of crown ethers to Li$^+$ in spent lithium-ion batteries leaching solutions, Chin. J. Chem. Phys. 32 (2019) 343, https://doi.org/10.1063/1674-0068/CJCP1809213.

[48] M.D. Hanwell, D.E. Curtis, D.C. Lonie, T. Vandermeersch, E. Zurek, G.R. Hutchison, Avogadro: an advanced semantic chemical editor, visualization, and analysis platform, J. Cheminformatics 2012 (4) (2012) 1–17, https://doi.org/10.1186/1758-2946-4-17.

[49] A.K. Rappe, C.J. Casewit, K.S. Colwell, W.A.G. III, W.M. Skiff, UFF, a full periodic table force field for molecular mechanics and molecular dynamics simulations, Journal of the American Chemical Society 114 (1992) 10024–10035, https://doi.org/10.1021/JA00051A040.

[50] F. Neese, F. Wennmohs, U. Becker, C. Riplinger, The ORCA quantum chemistry program package, J. Chem. Phys. 152 (2020), 224108, https://doi.org/10.1063/5.0004608.

[51] A.D. Becke, A new mixing of hartree-fock and local density-functional theories, J. Chem. Phys. 98 (1998) 1372, https://doi.org/10.1063/1.464304.

[52] F. Weigend, R. Ahlrichs, Balanced basis sets of split valence, triple zeta valence and quadruple zeta valence quality for H to Rn: design and assessment of accuracy, Phys. Chem. Chem. Phys. 7 (2005) 3297–3305, https://doi.org/10.1039/B508541A.

[53] Y. Sun, M. Zhu, Y. Yao, H. Wang, B. Tong, Z. Zhao, A novel approach for the selective extraction of Li$^+$ from the leaching solution of spent lithium-ion batteries using benzo-15-crown-5 ether as extractant, Sep. Purif. Technol. 237 (2020), 116325, https://doi.org/10.1016/j.seppur.2019.116325.

[54] Chr. Møller, M.S. Plesset, Note on an approximation treatment for many-electron systems, Physical Review 46 (1934) 618–622, https://doi.org/10.1103/PhysRev.46.618.

[55] A.V. Marenich, C.J. Cramer, D.G. Truhlar, Universal solvation model based on solute electron density and on a continuum model of the solvent defined by the bulk dielectric constant and atomic surface tensions, J. Phys. Chem. B 113 (2009) 6378–6396, https://doi.org/10.1021/jp810292n.

[56] S. Grimme, J. Antony, S. Ehrlich, H. Krieg, A consistent and accurate ab initio parametrization of density functional dispersion correction (DFT-D) for the 94 elements H-pu, J. Chem. Phys. 132 (2010) 154104, https://doi.org/10.1063/1.3382344.

[57] S. Kossmann, F. Neese, Efficient structure optimization with second-order many-body perturbation theory: the RIJCOSX-MP2 method, J. Chem. Theory Comput. 6 (2010) 2325–2338, https://doi.org/10.1021/CT100199K.

[58] F. Weigend, Accurate coulomb-fitting basis sets for H to Rn, Phys. Chem. Chem. Phys. 8 (2006) 1057–1065, https://doi.org/10.1039/B515623H.

[59] T. Lu, F. Chen, Multiwfn: a multifunctional wavefunction analyzer, J. Comput. Chem. 33 (2012) 580–592, https://doi.org/10.1002/jcc.22885.

[60] R.F.W. Bader, Atoms in Molecules: A Quantum Theory, Clarendon Press, 1994.

[61] L. Zhang, L. Li, H. Rui, D. Shi, X. Peng, L. Ji, X. Song, Lithium recovery from effluent of spent lithium battery recycling process using solvent extraction, J. Hazard. Mater. 398 (2020), 122840, https://doi.org/10.1016/j.jhazmat.2020.122840.

[62] G.R. Harvianto, S.G. Jeong, C.S. Ju, The effect of dominant ions on solvent extraction of lithium ion from aqueous solution, Korean J. Chem. Eng. 31 (2014) 828–833, https://doi.org/10.1007/s11814-014-0005-7.

[63] A. Masmoudi, G. Zante, D. Trébouet, R. Barillon, M. Boltoeva, Solvent extraction of lithium ions using benzoyltrifluoroacetone in new solvents, Sep. Purif. Technol. 255 (2021), 117653, https://doi.org/10.1016/j.seppur.2020.117653.

[64] L. Zhang, D. Shi, L. Li, X. Peng, F. Song, H. Rui, Solvent extraction of lithium from ammoniacal solution using thenoyltrifluoroacetone and neutral ligands, J. Mol. Liq. 274 (2019) 746–751, https://doi.org/10.1016/j.molliq.2018.11.041.

[65] G. Zante, M. Boltoeva, A. Masmoudi, R. Barillon, D. Trébouet, Highly selective transport of lithium across a supported liquid membrane, J. Fluor. Chem. 236 (2020), 109593, https://doi.org/10.1016/j.jfluchem.2020.109593.

[66] L. Zhang, L. Li, D. Shi, X. Peng, F. Song, F. Nie, Kinetics and mechanism study of lithium extraction from alkaline solution by HFTA and TOPO and stripping process using Lewis cell technique, Sep. Purif. Technol. 211 (2019) 917–924, https://doi.org/10.1016/J.seppur.2018.10.043.

[67] G.R. Harvianto, S.H. Kim, C.S. Ju, Solvent extraction and stripping of lithium ion from aqueous solution and its application to seawater, Rare Metals 35 (2016) 948–953, https://doi.org/10.1007/s12598-015-0453-1.

[68] L. Fabbrizzi, The origins of the coordination chemistry of alkali metal ions, ChemTexts 6 (2020) 1–19, https://doi.org/10.1007/s40828-020-0107-2.

[69] K. Momma, F. Izumi, in: IUCr, VESTA 3 for Three-dimensional Visualization of Crystal, Volumetric and Morphology Data 44, 2011, pp. 1272–1276, https://doi.org/10.1107/S0021889811038970. Urn: Issn: 0021-8898.

[70] E.F. Pettersen, T.D. Goddard, C.C. Huang, G.S. Couch, D.M. Greenblatt, E.C. Meng, T.E. Ferrin, UCSF chimera - a visualization system for exploratory research and analysis, J. Comput. Chem. 25 (2004) 1605–1612, https://doi.org/10.1002/jcc.20084.

[71] T. v Healy, Synergism in the solvent extraction of alkali metal ions by thenoyl trifluoracetone, J. Inorg. Nucl. Chem. 30 (1968) 1025–1036, https://doi.org/10.1016/0022-1902(68)80322-7.

[72] B.S. González, J. Hernández-Rojas, D.J. Wales, Global minima and energetics of Li$^+$(H$_2$O)$_n$ and Ca^{2+}(H$_2$O)$_n$ clusters for n ⩽ 20, Chem. Phys. Lett. 412 (2005) 23–28, https://doi.org/10.1016/J.cplett.2005.06.090.